Physics Letters B 692 (2010) 297–301

Contents lists available at ScienceDirect

Physics Letters B

www.elsevier.com/locate/physletb

Neutron-induced fission cross sections of short-lived actinides with the surrogate reaction method

G. Kessedjian [a], B. Jurado [a,*], M. Aiche [a], G. Barreau [a], A. Bidaud [a], S. Czajkowski [a], D. Dassié [a], B. Haas [a], L. Mathieu [a], L. Audouin [b], N. Capellan [b], J. Tassan-Got [b], J.N. Wilson [b], F. Berthoumieux [c], F. Gunsing [c], Ch. Theisen [c], O. Serot [d], E. Bauge [e], I. A

View metadata, citation and similar papers at core.ac.uk

[a] CENBG, CNRS/IN2P3, Univ. Bordeaux I, Chemin du Solarium B.P. 120, 33175 Gradignan, France
[b] IPN, CNRS/IN2P3, Univ. Paris-Sud, 91405 Orsay, France
[c] CEA Saclay, DSM/IRFU/SPhN, 91191 Gif-sur-Yvette cedex, France
[d] CEA-Cadarache, DEN/DER/SPRC/LEPh, 13108 Saint Paul lez Durance, France
[e] CEA DAM DIF, 91297 Arpajon, France
[f] Physics Division, Argonne National Laboratory, 9700 S. Cass Avenue, Argonne, IL 60439, USA

ARTICLE INFO

Article history:
Received 14 April 2010
Received in revised form 7 June 2010
Accepted 23 July 2010
Available online 30 July 2010
Editor: V. Metag

Keywords:
Surrogate reaction method
neutron-induced fission cross sections

ABSTRACT

Neutron-induced fission cross sections for ^{242,243}Cm and ^{241}Am have been obtained with the surrogate reaction method. Recent results for the neutron-induced cross section of ^{243}Cm are questioned by the present data. For the first time, the ^{242}Cm cross section has been determined up to the onset of second-chance fission. The good agreement at the lowest excitation energies between the present results and the existing neutron-induced data indicates that the distributions in spin and parity of states populated with both techniques are similar.

© 2010 Elsevier B.V. Open access under CC BY license.

Neutron-induced cross section data for short-lived nuclei are of great interest in applied and fundamental nuclear physics. For instance, fission and capture cross sections for short-lived actinides are important for nuclear waste transmutation using fast neutrons and for understanding element nucleosynthesis in astrophysics. However, such cross sections are difficult to measure directly as this requires producing and manipulating short-lived radioactive targets. These difficulties can be overcome with the so-called surrogate reaction technique, developed in the 1970s by Cramer and Britt [1], which consists in measuring the decay probability of a compound nucleus (e.g., fission, neutron emission, or radiative capture) produced via an alternative (surrogate) reaction, in this case a few-nucleon transfer reaction. The surrogate reaction is chosen such that the resulting nucleus has the same mass A and charge Z as the compound nucleus (CN) that results in the "desired" neutron-induced reaction. The neutron-induced cross section of nucleus A, $\sigma_{n,i}^{A}$ for decay channel "i" is then deduced from the product of the measured probability $P_i^{\exp}$ and the CN cross section for the neutron-induced reaction obtained from optical model calculations $\sigma_{\mathrm{CN}}^{\mathrm{cal}}$ as

$$\sigma_{n,i}^{A}(E_n) = \sigma_{\mathrm{CN}}^{\mathrm{cal}}(E_n) \cdot P_i^{\exp}(E_n). \quad (1)$$

In this Letter, we focus on fission cross section measurements. Thus, the exit channel of the surrogate reaction consists of a light ejectile and fission fragments. To determine the fission probability, the number of ejectiles detected in coincidence with the fission fragments is divided by the total number of ejectiles, the latter being labelled as "singles" events. The principle of the method is illustrated in Fig. 1. Recently, an alternative to the standard or "absolute" surrogate approach, called the surrogate ratio method (SRM) [2,3], has been developed. When applied to fission experiments, this method relates the ratio of two fission cross sections to a ratio of ejectile–fission coincident events from two surrogate reactions. The advantage of the SRM is that it removes the need to measure the total number of reaction events, i.e., the "singles" events which, as shown below, eliminates an important source of systematic uncertainty. However, the SRM requires one of the fission cross sections to be known in order to infer the desired one. In addition, the two surrogate reactions should be sufficiently similar; i.e., the projectile–ejectile combination should be the same and the compound nuclei should be close enough in A and Z to have similar properties [4]. This implies severe limitations when one is interested in a region dominated by radioactive nuclei, such as Am and Cm isotopes, for which both data and targets are rather scarce.

* Corresponding author.
E-mail address: jurado@cenbg.in2p3.fr (B. Jurado).

0370-2693 © 2010 Elsevier B.V. Open access under CC BY license.
doi:10.1016/j.physletb.2010.07.048

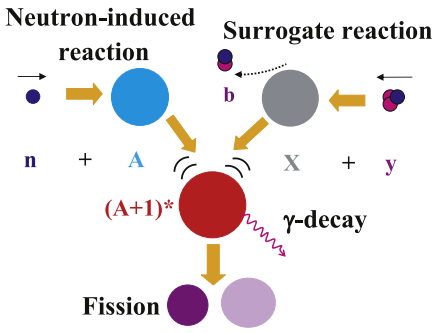

Fig. 1. (Color online.) Schematic representation of the surrogate method. In this case, the surrogate reaction is a transfer reaction X(y, b)$A+1$. Two possible decay modes (fission and gamma emission) of the excited compound nucleus $(A+1)^*$ are represented.

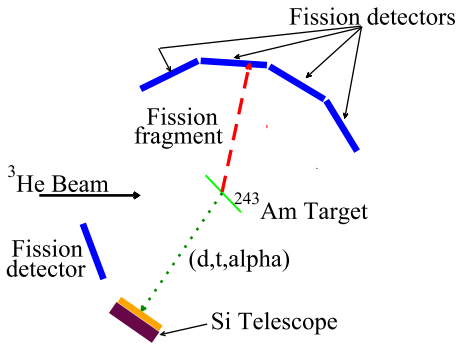

Fig. 2. Top view of the set-up for the fission probability measurements.

An important issue to be investigated in the context of surrogate reactions is the difference between the distributions in spin and parity (J^π) of the states populated in the desired and surrogate reactions, a problem referred to as the "J^π population mismatch" in the literature [4,5]. Since the J^π population influences the decay probabilities of the CN, one would a priori expect differences between the decay probabilities measured in surrogate and in neutron-induced experiments. However, in the Weisskopf–Ewing limit, the decay probability is independent of the spin and parity of the CN and Eq. (1) is valid. The conditions under which the Weisskopf–Ewing limit applies have been investigated in Refs. [4,5]. It was stated in Ref. [4] that this limit holds when (i) the excitation energy is sufficiently high for the decay widths to be dominated by the statistical level density, and when (ii) the angular momentum of the CN is not much larger than the spin-cutoff parameter of the level density distribution, which, for the actinide region, is about $7\hbar$. Clearly, the comparison between cross sections measured with the surrogate method and those obtained directly with neutrons at low energies should provide information on possible differences between the J^π distributions achieved in the two methods. Indeed, at the lowest energies corresponding to the fission threshold, this mismatch could be revealed by transition states near the top of the fission barriers whose feeding could be dependent on the entrance channel. The greatest effect is expected for even–even heavy systems which cross the fission barriers through a few collective states. Nevertheless, and because of a larger density, these transition states should be less important for odd–odd systems. Discrepancies between surrogate and neutron-induced data have been attributed to the J^π population mismatch in Refs. [3,5].

The present collaboration has already applied the surrogate technique to the measurement of the neutron-induced fission [6] and capture [7] cross sections of ^{233}Pa ($T_{1/2} = 27$ day). In the present work, the surrogate reaction method is used to determine the neutron-induced fission cross sections of ^{242}Cm($T_{1/2} =$ 162.8 day), ^{243}Cm($T_{1/2} = 29.1$ yr) and ^{241}Am($T_{1/2} = 432.2$ yr). These cross sections are of interest for nuclear waste transmutation. However, in the case of the Cm isotopes, the available data are rather scarce or inconsistent and the international evaluations used for reactor simulations present important differences. To reach and study these nuclei we have employed few-nucleon transfer reactions using a ^{3}He projectile on a ^{243}Am($T_{1/2} = 7370$ yr) target. Two targets, of approximately 100 μg/cm^2 thickness, were prepared at the Argonne National Laboratory, each deposited on a 75 μg/cm^2 carbon backing. ^{3}He beams of 24 and 30 MeV were provided by the Tandem accelerator at the IPN Orsay.

The ^{3}He-induced transfer reactions on the ^{243}Am target lead to the production of various heavy residues. Table 1 lists the transfer channels considered in the present experiment, and the corresponding neutron-induced reactions that were obtained with the surrogate method as a result. The advantage of using transfer reactions is clear: the simultaneous access to several transfer channels allows one to determine cross sections for various nuclei from a single projectile-target combination. Moreover, since there are two bodies in the outgoing reaction channel, the excitation energy of the heavy nucleus E^* follows a broad probability distribution. The CN excitation energy is related to the neutron energy, E_n, via the relation $E^* = B_n + (A-1) \times E_n/A$, where B_n is the neutron binding energy in the CN. Therefore, for a fixed beam energy, the surrogate method enables the determination of cross sections over a wide range of corresponding neutron energies. The same set of nuclei was investigated in the pioneering work of Gavron et al. [8]. However, the aim of that measurement was the extraction of fission barrier heights and curvatures from the onset of the measured fission probabilities rather than the determination of neutron-induced fission cross sections.

Table 1
Transfer channels investigated in the reaction ^{3}He + ^{243}Am and the corresponding neutron-induced fission reactions.

Transfer channel	Neutron-induced reaction
^{243}Am(^{3}He, d) ^{244}Cm	^{243}Cm(n, f)
^{243}Am(^{3}He, t) ^{243}Cm	^{242}Cm(n, f)
^{243}Am(^{3}He, α) ^{242}Am	^{241}Am(n, f)

The set-up used to determine the fission probability of the compound nuclei formed after a transfer reaction is displayed in Fig. 2. Two Si telescopes, placed at 130° (angular aperture ±4°) with respect to the beam axis, served to identify the ejectiles. If the corresponding heavy residue undergoes fission, one of the fragments was detected in coincidence by means of a fission-fragment multidetector consisting of 15 photovoltaic cells distributed among 5 units, each composed of 3 cells placed vertically above one another. Four units were located in the forward direction with an angular coverage of 14° to 125°. The fifth was positioned at 180° from the foremost unit. In this way, the fission fragments hitting the foremost unit were detected in coincidence with their complementary fragment in one of the cells of the fifth one. The determination of the kinetic energies of the two fragments in a given fission event provides a means to infer the fragment mass distribution. Results on the latter distribution will be presented in a forthcoming publication. The fifth unit also provided a data point at backward angles for the angular distribution. More details on the experimental set-up can be found in Ref. [6]. The identification of the light charged particles and the determination of their energy and scattering angle was achieved in the Si telescopes. With this information and the related Q-values, the excitation energy E^* of the corresponding compound nuclei was determined. The

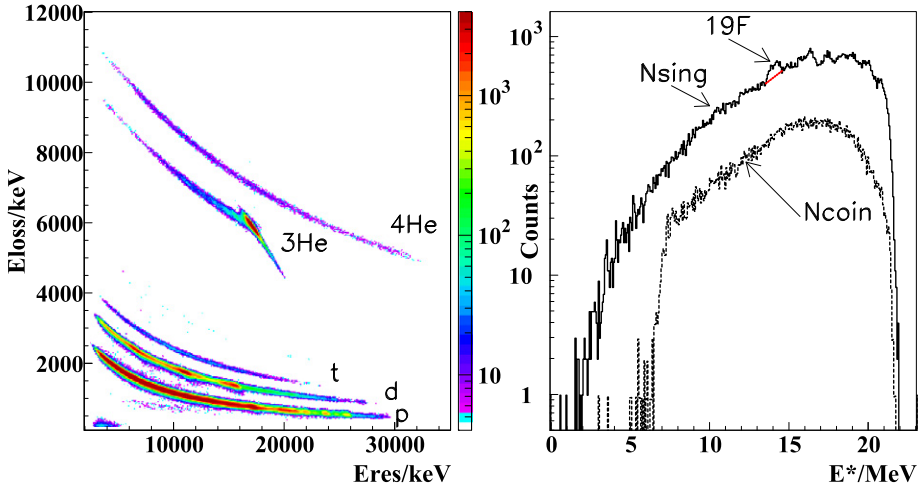

Fig. 3. Left: Energy loss versus residual energy in one of the Si telescopes. Right: Number of tritons as a function of the ^{243}Cm excitation energy. The interpolation of the singles spectrum under the ^{19}F contaminant peak is represented by the red dotted line (see text for details). (For interpretation of the references to color in this figure legend, the reader is referred to the web version of this Letter.)

left panel of Fig. 3 illustrates the identification achieved in one of the telescopes through the conventional energy loss *vs* residual energy plot. By selecting one type of light particle, for example tritons t, the spectrum represented by the solid line on the right of Fig. 3, the so-called "singles" spectrum N_{sing}, is obtained. It represents the number of tritons, i.e., the number of ^{243}Cm nuclei, as a function of their excitation energy. The broad peaks at the highest excitation energies in the spectrum stem from transfer reactions on the carbon backing and on ^{19}F impurities in the target. The background from reactions on carbon was measured separately and subtracted from the singles spectrum. The resulting singles spectrum was interpolated under the ^{19}F peaks, introducing an additional source of uncertainty. This systematic error represents at most a 4% contribution to the overall uncertainty. By selecting the tritons detected in coincidence with a fission event, the spectrum associated with the number of ^{243}Cm nuclei that have undergone fission, N_{coin}, is obtained (see dashed line in the right panel of Fig. 3). The ratio between the N_{coin} and N_{sing} spectra, corrected for the fission detector efficiency $E_{\text{ff}}(E^*)$, gives the fission probability of ^{243}Cm as a function of the excitation energy; i.e., $P_{\text{f}}(E^*) = N_{\text{coin}}(E^*)/(N_{\text{sing}}(E^*) \times E_{\text{ff}}(E^*))$. The geometrical efficiency of the fission detector was approximately 47%, and was calculated with a Monte-Carlo simulation that also reproduced the experimental efficiency determined from a measurement with a ^{252}Cf source. With this Monte-Carlo simulation, it is possible to calculate the effective efficiency for each E^* bin. The effect of the fission-fragment angular anisotropy on the detector efficiency amounts to a 2–3% correction at most. Our results for the fission probabilities are in general good agreement with the ones of Ref. [8]. However, our data extend to higher E^*. The maximum neutron energies considered in [8] for compound nuclei ^{242}Am and ^{243}Cm are 6.2 and 5.8 MeV, respectively, instead of 10 MeV in our case. For ^{244}Cm, our results are below those of Ref. [8] between 2 and 3 MeV. Nevertheless, this difference is 15% at most and is well within the error bars of the two measurements.

The measured fission probabilities of ^{244,243}Cm and ^{242}Am were translated into the associated neutron-induced fission cross sections by multiplying the experimental fission probability with the corresponding calculated CN cross section. The latter was obtained with a Lane-consistent semi-microscopic [9] deformed [10] optical model potential built using deformed radial nuclear densities calculated in the Hartree–Fock–Bogoliubov framework with the Gogny D1S interaction [11]. The error associated with the CN cross section is estimated to be $\sim 10\%$. The results for the three surrogate reactions under investigation are displayed in Figs. 4, 5 and 6. The final error on the reported cross sections is 11% on average and reaches 14% in regions with low statistics. A detailed description of how different sources of errors were considered will be presented in a forthcoming paper. The binning size for the data is 210 keV.

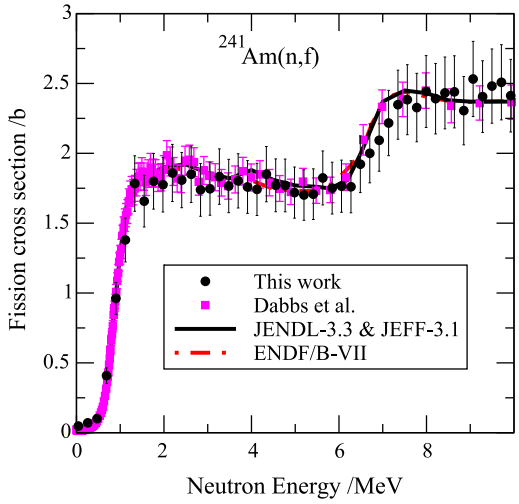

Fig. 4. (Color online.) Fission cross section for ^{241}Am as a function of neutron energy compared with neutron-induced data and the evaluations from several international libraries.

As shown in Fig. 4, the measured ^{241}Am(n,f) cross section is in good agreement with the data by Dabbs et al. [12] and with the available evaluations JENDL [13], JEFF [14] and ENDF/B-VII [15]. We have chosen the data by Dabbs et al. [12] among all the other neutron-induced data for ^{241}Am because they cover a broad range in neutron energies, they represent the shape of the majority of the data rather well and they are commonly used for evaluations. Fig. 5 presents the results for ^{242}Cm(n,f) in comparison with the data by Vorotnikov et al. [16]: there is good agreement between both sets in this case as well. For neutron energies larger than 1.4 MeV, no other neutron-induced data exist. This presumably accounts for the important discrepancies between evaluations based on various international libraries in this energy range, although the JENDL and JEFF libraries present the best overall agreement with the data. The ^{243}Cm(n,f) cross section can be found in Fig. 6. Due

to the presence of contaminant peaks, the maximum neutron energy extracted in this case is 3 MeV. The results are compared with the most recent measurements by Fomushkin et al. [17] and by Fursov et al. [18]. At the lowest neutron energies, the agreement between the three measurements is rather satisfactory. Beyond 0.7 MeV, however, the present data follow those of Ref. [17] fairly well, but they clearly deviate from those of Ref. [18]. Concerning the libraries, JENDL closely follows Ref. [18] above 0.7 MeV. ENDF is in satisfactory agreement with the present data above 0.7 MeV and JEFF is compatible with our data and Ref. [17] only between 0.5 and 1.8 MeV. The cross sections of Ref. [18], in the 1 to 3 MeV energy range, are significantly higher than those measured for neighboring fissile isotopes such as ^{245}Cm [19,20] and ^{247}Cm [18], which are all below 2 barns. Moreover, under the reasonable assumption that the neutron inelastic scattering cross section on ^{243}Cm ranges from 1 to 1.5 barns at 2 MeV neutron energy, the value of the fission cross section of 2.6 barns obtained in Ref. [18] at 2 MeV would result in a total compound cross section (neglecting the capture contribution) varying from 3.6 to 4.1 barns, a value considerably larger than the 3 barns predicted by optical model calculations [9,10]. All these arguments suggest that the results in Ref. [18] (and, hence, the JENDL evaluation) overestimate the ^{243}Cm(n, f) cross section at neutron energies between 0.7 MeV and 3 MeV.

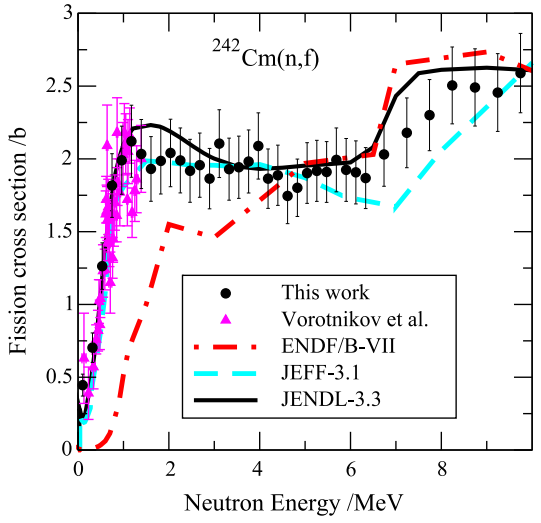

Fig. 5. The same as in Fig. 4, but for ^{242}Cm.

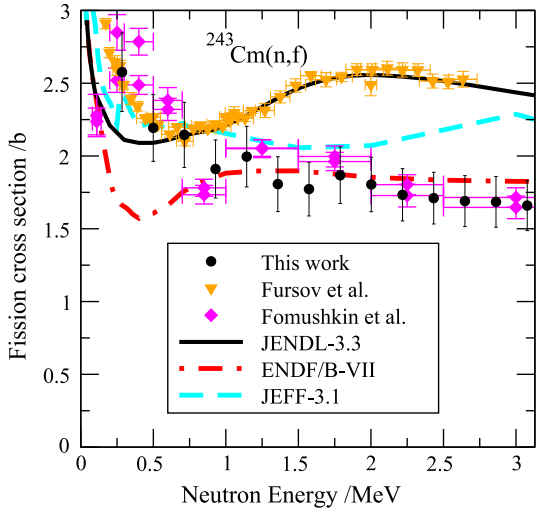

Fig. 6. The same as in Fig. 4, but for ^{243}Cm.

Fig. 7 illustrates in detail the low neutron-energy part of Figs. 4, 5 and 6. The binning size of our data is bigger than the one of the neutron-induced measurements. However, Fig. 7 indicates that, for all three nuclei, the surrogate reaction data reproduce very well the general trend of the neutron cross sections and no systematic discrepancies are observed between the present results and the neutron-induced measurements at the lowest energies. This good agreement is particularly interesting in the case of the even–odd ^{243}Cm and even–even ^{244}Cm compound nuclei, as it indicates that the J^π distributions of the states populated through the transfer reactions used in this work are similar to those of the levels fed in the corresponding neutron-induced reactions. This absence of J^π effects is at variance with the J^π distribution disparities suggested for CN ^{237}U in Ref. [3], and with Ref. [5], where the J^π distribution populated in the ^{234}U(t, p) reaction was corrected in order to reproduce the ^{235}U(n, f) data. Note, however, that the fissioning nuclei considered in Refs. [3,5] are lighter than the ones studied here.

In summary, the surrogate reaction method was used to determine the neutron-induced fission cross sections of three short-lived actinides. The deduced ^{241}Am(n, f) and ^{242}Cm(n, f) cross sections agree with the available data obtained via neutron-induced reactions. The new results for the fission cross section of ^{242}Cm extend up to the onset of second-chance fission. None of the existing neutron-induced fission data for ^{242}Cm reached as high in neutron energy. For the ^{243}Cm(n, f) cross section, the present results are in good agreement with the existing neutron-induced data at the

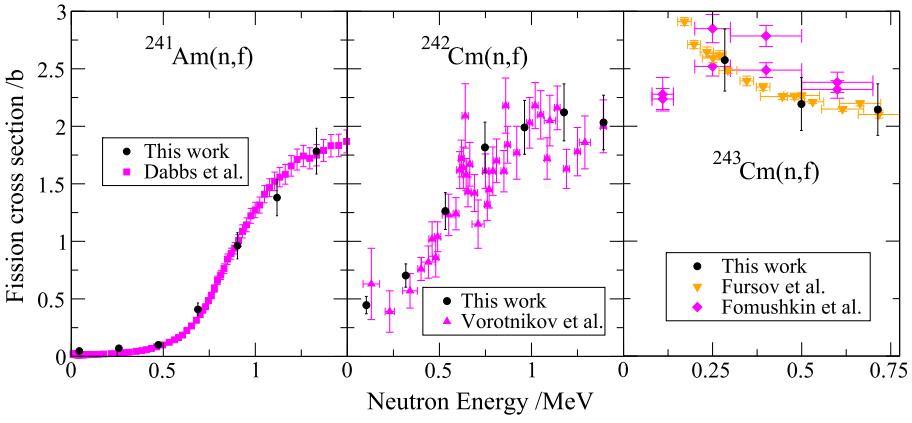

Fig. 7. (Color online.) Fission cross sections as a function of neutron energy.

lowest neutron energies, but are clearly below the recent data of Fursov et al. [18] beyond 0.7 MeV. The good agreement observed at the lowest neutron energies between the present results and the neutron-induced data for ^{242}Cm(n, f) and ^{243}Cm(n, f) indicates that the population of excited states generated by the transfer reactions used in this work is similar to the distribution fed in neutron-induced reactions. This agreement illustrates the potential of the surrogate reaction method to provide neutron-induced fission cross sections for short-lived nuclei. Further experimental and theoretical efforts are, however, required to extend the use of this powerful technique to other types of cross sections such as radiative capture as well as to asses and understand the limits of its application.

Acknowledgements

We thank the tandem accelerator staff and the target laboratory of the IPN Orsay for their support during the experiment. This work was partly supported by the CNRS program PACEN/GEDEPEON, the Conseil Régional d'Aquitaine, the US Department of Energy, Office of Nuclear Physics, under contract DE-AC02-06CH11357. The authors are also indebted for the use of ^{243}Am to the Office of Basic Energy Sciences, US Department of Energy, through the transplutonium element production facilities at Oak Ridge National Laboratory.

References

[1] J. Cramer, H. Britt, Nucl. Sci. Eng. 41 (1970) 177.
[2] C. Plettner, et al., Phys. Rev. C 71 (2005) 051602(R).
[3] B.F. Lyles, et al., Phys. Rev. C 76 (2007) 014606.
[4] J. Escher, F.S. Dietrich, Phys. Rev. C 74 (2006) 054601.
[5] W. Younes, H.C. Britt, Phys. Rev. C 67 (2003) 024610.
[6] M. Petit, et al., Nucl. Phys. A 735 (2004) 345.
[7] S. Boyer, et al., Nucl. Phys. A 775 (2006) 175.
[8] A. Gavron, et al., Phys. Rev. C 13 (1976) 2374.
[9] E. Bauge, J.P. Delaroche, M. Girod, Phys. Rev. C 63 (2001) 024607.
[10] E. Bauge, et al., Phys. Rev. C 61 (2000) 034306.
[11] J.F. Berger, M. Girod, D. Gogny, Comput. Phys. Commun. 63 (1991) 365.
[12] J.W.T. Dabbs, et al., Nucl. Sci. Eng. 83 (1983) 2.
[13] K. Shibata, et al., J. Nucl. Sci. Technol. 39 (2002) 1135.
[14] JEFF report 21, OECD/NEA No. 6190 (2006), ISBN 92-64-02314-3.
[15] M.B. Chadwick, et al., Nucl. Data Sheets 107 (2006) 2931.
[16] P.E. Vorotnikov, et al., Yadern. Fiz. 40 (1984) 1141.
[17] E.F. Fomushkin, et al., At. Energ. 69 (1990) 258.
[18] B.I. Fursov, et al., in: Conf. Nucl. Data for Sci. and Techn., Trieste, 1997, p. 488.
[19] E.F. Fomushkin, et al., At. Energ. 63 (1987) 242.
[20] R.M. White, et al., in: Conf. Nucl. Data for Sci. and Techn., Antwerp, 1982, p. 218.